Effects of Pioglitazone on Promoting Energy Storage, not Expenditure, in Brown Adipose Tissue of Obese *fa/fa* Zucker Rats: Comparison to CL 316,243

Bryan F. Burkey, Mei Dong, Karen Gagen, Michele Eckhardt, Nancy Dragonas, Wei Chen, Paul Grosenstein, Greg Argentieri, and Christopher J. de Souza

Recent advances in the treatment of non–insulin-dependent diabetes mellitus (NIDDM) include the use of thiazolidinediones (TZDs), agents that enhance insulin action, in part, through an activation of adipose tissue peroxisome proliferator-activated receptor gamma. Current evidence also indicates that these agents upregulate uncoupling protein 1 (UCP1) gene expression in brown adipocytes and increase interscapular brown adipose tissue (IBAT) mass in rodents, suggestive of a thermogenic component to their mechanism of action. In the present study, the TZD pioglitazone (PIO) and the β_3-adrenoceptor agonist CL 316,243 (CL), were used to determine whether the antidiabetic effects of PIO, like those of CL, may, in part, be mediated by an increase in either IBAT thermogenesis or whole-body energy expenditure. Treatment of obese, insulin resistant *fa/fa* Zucker rats with PIO for 10 days resulted in a 2- to 3-fold increase in IBAT mass, due largely to an increase in adipocyte size and number, and increased fatty acid biosynthesis. However, unlike the effects of CL, the PIO-induced IBAT changes were not associated with an increase in UCP1 expression or whole-body energy expenditure. In contrast to CL, PIO substantially increased body weight gains over the 10-day treatment period by increasing feeding efficiency. These data suggest that, unlike CL, the actions of PIO in the obese Zucker rat does not include increased energy expenditure, but rather strengthens its role as an adipogenic and lipogenic agent, which promotes energy storage.

INSULIN RESISTANCE is a hallmark of obesity, which in the presence of dysfunctional β-cell insulin secretion, leads to type 2 diabetes mellitus. The discovery and development of the thiazolidinediones (TZDs) as insulin sensitizers have lead to a new line of therapy for the treatment of type 2 diabetes.[1] Preclinical and clinical studies show that these agents enhance insulin action and improve glycemic control primarily by increasing peripheral glucose disposal and reducing hepatic glucose output. Adipose tissue is believed to be a primary target based on the observations that the TZDs bind and activate peroxisome proliferator-activated receptor-gamma (PPAR-γ), a nuclear hormone receptor expressed at high levels in adipose tissue. While PPAR-γ activation has been shown to correlate well with in vivo glucose lowering,[2] the means by which this action translates to improved whole-body insulin sensitivity remain unclear.

Adipose tissue is a key regulator of whole-body energy metabolism, where it plays a central role in the balance between energy storage and energy mobilization. In vitro, the TZDs stimulate adipocyte differentiation and increase the expression and activity of lipogenic enzymes.[3,4] In vivo, such adipogenesis is expected to lead to an increase in the number of small, insulin-sensitive adipocytes that have a higher propensity for energy storage, especially free fatty acid (FFA) uptake and reesterification. A reduction of FFA availability should, in turn, result in improved whole-body insulin sensitivity.[5] Consistent with these anabolic actions are the observations that these agents promote weight gain in rodent models.[6-10] However, clinical studies have not shown substantial weight gain, leaving open the issue of whether the TZDs work primarily by increasing energy storage in the form of increased adiposity or whether they mediate their effects via alternative mechanisms.

Other than energy storage, another approach to improve glucose homeostasis is to promote energy expenditure.[11,12] In rodents, activation of β_3-adrenoceptors with CL 316,243 (CL) stimulates brown adipose tissue (BAT) thermogenic activity by increasing the activity and expression of uncoupling protein 1 (UCP1), resulting in an uncoupling of oxidative phosphorylation and the dissipation of energy in the form of heat. The actions of CL in rodent models lead to improved glucose homeostasis,[13-16] an action attributed largely to the compounds effects on adipose tissue depots,[15,16] where FFAs are mobilized from white adipose depots and serve as an energy source for BAT thermogenesis.

Recent reports suggest that the antidiabetic TZDs may also promote energy expenditure, which like the β_3-adrenoceptor agonists, would then lead to improved glucose homeostasis. In rodents, the TZDs increase interscapular BAT (IBAT) mass,[17,18] while in vitro they stimulate the differentiation of preadipocytes into brown adipocytes as determined by the presence of UCP1 gene expression.[18-21] This is especially relevant because it suggests that the TZDs may have the potential to promote the formation of brown adipocytes in human white adipose tissue (WAT) and thereby increase energy disposal through the formation of heat. Hence, the aim of the present study was to determine whether the antidiabetic effects of the TZDs, like those of the β_3-adrenoceptor agonists, might, in part, be mediated via the activation of the IBAT through an increase in energy expenditure and thermogenic activity. To do so, the TZD pioglitazone (PIO) and the rodent-specific β_3-adrenoceptor agonist CL-316,243, either alone or in combination, were administered to chronically obese female Zucker (*fa/fa*) rats to assess their effects on IBAT physiology and whole-body metabolism.

From the Department of Metabolic and Cardiovascular Diseases, Summit, and Pathology, East Hanover, NJ. Novartis Biomedical Research Institute, Novartis Pharmaceutical Corp, Summit, NJ; and the Department of Pathology, Novartis Pharmaceutical Corp, East Hanover, NJ.

Submitted October 20, 1999; accepted April 9, 2000.

Address reprint requests to Bryan F. Burkey, PhD, Novartis Institute of Biomedical Research, 130-3319, 556 Morris Ave, Summit, NJ 07901-1398.

0026-0495/00/4910-0019$10.00/0
doi:10.1053/meta.2000.9524

MATERIALS AND METHODS

Animal Studies

Female fatty Zucker (*fa/fa*) rats and their lean (FA/?) littermates were purchased from Charles River Labs (Wilmington, MA) at 10 weeks of age. All procedures in this study were in compliance with the Animal Welfare Act Regulations 9 CFR Parts 1, 2, and 3, and the "Guide for the Care and Use of Laboratory Animals" (National Institutes of Health, 1985). The animals had free access to powdered rodent chow (Purina Rodent Chow 5001; W.F. Fisher, Inc, Boundbrock, NJ) and water and were maintained at 21 ± 1°C on a 12:12 hour light:dark reverse phase photoperiod. (lights on from 6 PM to 6 AM). After a 4-week entrainment period, osmotic mini-pumps (Alzet, model 2002) were implanted subcutaneously, in the dorsal lumbar region, under isoflurane anesthesia (Fort Dodge Animal Health, Fort Dodge, IA). The mini-pumps delivered either saline or CL 316,243 in saline at 1 mg/kg/d for up to 11 days. PIO was administered as an admixture in normal rodent chow (0.4 mg/g) that was set to deliver a dosage of 20 mg/kg/d. Body weights and food consumption were measured daily over the 10-day treatment period. Based on body weight and food consumption data, the PIO group received an average PIO dose of 30.3 ± 0.4 mg/kg/d and the PIO + CL group 21.9 ± 1.7 mg/kg/d. Metabolic rates (MR) were measured using an open circuit respirometer (Columbus Instruments, Columbus, OH) during which time the animals had free access to food and water. After a 120-minute acclimation period, volumes of oxygen consumed and carbon dioxide produced were determined once every 10 to 12 minutes and converted to standard temperature and pressure. The MR was calculated using the equation by Weir.[22]

Oral Glucose Tolerance Test and Tissue Collection

On day 11, after a 12-hour fast, animals were administered a 1.35 g/kg glucose bolus orally, and blood samples were obtained via a tail nick at −10, 0, 15, 30, 45, 60, and 120 minutes postglucose dose. After a 2-hour recovery period, the animals were anesthetized (50 mg/kg sodium pentobarbital, intraperitoneal [IP]), the interscapular region exposed, and brown adipose tissue cleaned of surrounding white adipose, muscle, and connective tissue while still being perfused. The cleaned tissue was then rapidly removed, weighted, and pieces taken fresh for adipocyte isolation, fixed for histology, or snap-frozen in liquid nitrogen for biochemical and RNA analysis.

Plasma Metabolites

Plasma glucose concentrations were determined using a glucose analyzer (YSI-2700, Yellow Springs Instruments, Yellow Springs, OH). Plasma insulin levels were determined with a double antibody radioimmunoassay technique using a rat-specific insulin antibody (Linco Research, St Louis, MO). Plasma free FFAs were determined colormetrically using a nonesterified FFA kit (WACO Pure Chemicals, Richmond, VA).

Preparation and Sizing of Adipocytes

Freshly isolated rat brown adipocytes were prepared as previously described[23,24] with slight modifications. Briefly, the BAT sample was placed in a wide-mouth 30 mL polyethylene bottle containing 4 mL of Krebs-Ringer-Phosphate-Hepes (KRPH) buffer (130 mmol/L NaCl, 4.7 mmol/L KCl, 2.5 mmol/L $CaCl_2$, 1.24 mmol/L $MgSO_4$, 2.5 mmol/L NaH_2PO_4, 10 mmol/L Hepes) with 5% bovine albumin (Intergen, Purchase, NY, Bovuminar Cohn Fraction V), 1.0 mg/mL of collagenase (Worthington Biochemicals, Freehold, NJ), and 0.6 mmol/L D-glucose (pH 7.4). The tissue was then minced using sharp scissors and the bottle shaken at 140 cycles/minute in a 37°C water bath for 40 to 70 minutes. The digested tissue was passed through a nylon filter (250 µm Nitex, Tetko Inc, Depew, NY), and the flow-through cell suspension was washed 3 times with KRPH containing 5% bovine albumin at pH 7.4. The resulting cell suspension (approximately 20% vol/vol) was maintained in KRPH wash buffer with constant shaking at 40 cycles/minute in the 37°C water bath until use. Adipocyte number and size distribution were performed on these freshly isolated adipocytes using a Coulter Counter equipped with a 400 µm orifice tube, a stirred sample chamber, and a multichannel particle analyzer (Multisizer II, Coulter Electronics, Miami, FL). Adipocytes were diluted into 25 mL of electrolyte solution (Isoton II containing 10% glycerol) and stirred to maintain an even suspension. Cell number and size profiles were generated using the siphon option with the manometer set for 2 mL, and adipocyte diameters were distributed across 256 channels. Using the Accucomp software (Coulter Electronics, Miami, FL) supplied with the Multisizer II, analysis of adipocyte size distributions were performed on cells ranging between 20 and 200 µm in diameter and expressed as a percent of the total population.

Tissue Homogenates and Biochemical Analysis

Weighed pieces (80 to 300 mg) of freeze-clamped tissue (stored at −80°C) were added to 1 mL of ice-cold homogenization buffer (100 mmol/L potassium phosphate, 250 mmol/L sucrose, 2 mmol/L EDTA, 1 mmol/L Hepes, pH 7.0) and homogenized for approximately 30 seconds on high speed using a Brinkman Polytron PT3000 homogenizer (Brinkman Instruments, Westbury, NY). Tissue components were extracted by 3 cycles of freeze-thawing (liquid nitrogen/37°C) and then centrifuged at 4,000 rpm for 5 minutes at 4°C. The cleared supernatant were collected and stored at −80°C until all samples were processed and analysis could be performed for protein, DNA, citrate synthase activity, and fatty acid synthase activity. Protein concentrations were determined using the *DC* Protein Assay (Bio-Rad, Hercules, CA). DNA was measured using the PicoGreen dsDNA Quantitation Kit (Molecular Probes, Eugene, OR). Citrate synthase activity was measured in the tissue extracts as a marker of tricarboxylic acid (TCA) cycle activity according to the method of Srere et al[25] and adapted to a 96-well plate format. Briefly, each tissue extract was serially diluted in 0.1 mol/L Tris(hydroxymethyl)aminomethane-HCl (pH 7.8), and 10 µL was added to 190 µL of a buffer containing 100 mmol/L Tris-HCl (pH 7.4), 50 µmol/L acetyl-CoA, 100 µmol/L oxaloacetate, and 100 µmol/L dithiobis(2-nitrobenzoic acid). The production of mercaptide ion was monitored kinetically at 405 nm for 10 minutes using a Molecular Devices Thermomax spectrophotometer set at 30°C. Fatty acid synthase (FAS) activity was measured in tissue extracts by a modification of previous methods[26,27] and adapted to a 96-well format. Briefly, each tissue extract was serially diluted (up to 8-fold) in a buffer containing 0.1 mol/L potassium phosphate, pH 6.5, where 60 µL was added to 140 µL of 150 µmol/L nicotinamide adenine dinucleotide phosphate (NADPH) and 120 µmol/L acetyl CoA followed by a 10-minute incubation at 30°C. To start the reaction, 20 µL of 1.17 µmol/L malony CoA was added and the kinetics of NADPH consumption followed at 340 nm for 15 minutes at 30°C.

RNA Isolation and Northern Analysis

Total cellular RNA was extracted from BAT using the Promega RNAgents kit (Madison, WI). To obtain a cDNA probe for rat UCP1, mRNA was isolated from total RNA using Oligotex mRNA Maxi kit (Qiagen, Santa Clarita, CA), and first strand cDNA was synthesized using a cDNA Synthesis kit from Boehringer Mannheim (Indianapolis, IN) followed by second strand synthesis. The rat UCP1 cDNA fragment (882 bp) was obtained by polymerase chain reaction (PCR) using rat BAT cDNA as a template and primers based on the Gene Bank sequence M-11814 (forward, 5′-GAGTTCGGTACCCACATCAGG-3′ and reverse 5′-GCATAGGAGCCCAGCATAGG-3′). The mouse leptin cDNA fragment (504 bp) was obtained by PCR using mouse WAT cDNA as a template and primers based on the Gene Bank sequence U18812 (forward, 5′-GCGAATTCTCAGCATTCAGGGCTAACATC-3′ and re-

verse 5′-GCGAATTCATGTGCTGGAGACCCCTGTG-3′). Northern analysis was performed by fractionating total RNA on a 1.2% agarose gel containing formaldehyde and transferred to Hybond N^+ nitrocellulose (Amersham, Arlington Heights, IL) and crosslinked. The cDNA probes were random-prime labeled with [^{32}P]deoxycytidine triphosphate (dCTP) (Amersham) using the Redi-prime kit (Amersham). The blots were prehybridized with Rapid-hyb buffer (Amersham) for 1 hour at 65°C, then the labeled probes were added and hybridized overnight at 65°C. Blots were washed once for 20 minutes at room temperature with 1× SSC containing 0.5% sodium dodecyl sulfate (SDS) and 3 times for 20 minutes at 68°C with 0.2 × SSC containing 0.5% SDS. Detection of labeled blots was performed using a Storm Phosphoimager (Molecular Dynamics, Sunnyvale, CA).

Histology and Electron Microscopy

Samples were taken from IBAT tissue (the center of the organ), fixed in 0.9% saline containing 50 mmol/L collidine and 2% osmium tetroxide (Sigma, St Louis, MO) for 24 hours. Small pieces (1 mm^2) were selected, rinsed in cacodylate buffer, dehydrated through an upgraded ethanol series, and embedded in EMbed (Epon) 812 in flat silicon molds. Ultrathin sections, double-stained with uranyl acetate and lead citrate, were examined using a Zeiss EM-902 transmission electron microscope (TEM; Carl Zeiss, Inc, Thornwood, NY). A total of 2 to 3 tissue blocks were processed for each treatment group and surveyed by TEM using an unbiased sampling method. Micrographs were taken at 1,100 magnification, and 1 representative micrograph per treatment group selected.

Unless otherwise stated, data are presented as mean ± SE, and statistical analysis was performed by 1-way analysis of variance (ANOVA) with a Student-Newman-Keuls post ANOVA test using SigmaStat v2.0 (Jandel Scientific, San Ralael, CA).

RESULTS

The antidiabetic effects of both PIO and CL were assessed in obese female *fa/fa* Zucker rats (Table 1). When compared with their lean littermates, the obese control rats were mildly hyperglycemic with markedly elevated fasting plasma insulin (10 times), and FFA (3 times) levels, and a greatly diminished glucose tolerance, all indicative of profound insulin resistance. Both PIO and CL were equally efficacious at reducing fasting plasma insulin (56% and 62%, respectively) and FFA (59% and 37%, respectively) levels, and at restoring glucose tolerance to levels comparable to those in lean controls. In combination, PIO and CL did not work either additively or synergistically to further decrease fasting plasma insulin or FFA levels. In these mildly hyperglycemic animals, only PIO decreased fasting plasma glucose to levels seen in the lean animals.

While both agents had similar antidiabetic effects, their effects on body weight were opposite (Table 1). When compared with controls, PIO treatment doubled the rate of weight gain (Δ 31 ± 2 g *v* Δ 71 ± 3 g, $P < .05$), while CL treatment reduced weight gain by one half (Δ 14 ± 5 g, $P < .05$). The increase in body weight gain in the PIO group was associated with an increase in food consumption. However, the reduced weight gain in the CL group was independent of food consumption, indicative of an increase in energy expenditure. When given in combination, the opposite effects of the 2 compounds resulted in an intermediate, but modestly higher body weight gain (Δ 45 ± 5 g), which was significantly different from the weight changes when either compound was administered individually. While the PIO + CL group consumed 25% less pioglitazone as an admixture with food, both the PIO and PIO + CL group received at least the targeted dose of 20 mg/kg/day, that is above the dose that is maximally efficacious.

When expressed as an index of feeding efficiency (Δ body weight gain/total food consumption, Table 1), PIO almost doubled feeding efficiency, showing greater body weight gain for the amount of food consumed. In contrast, CL decreased feeding efficiency to levels significantly lower than in the controls. When given in combination, the effect of PIO on feeding efficiency dominated.

In rats, BAT is a major site of thermogenic activity. PIO treatment resulted in a 172% increase in IBAT mass after 10 days of treatment (Table 2). On dissection, the appearance of IBAT from PIO-treated animals was similar to that from the control, more closely resembling the appearance of WAT than that of BAT. In contrast, CL treatment had no effect on IBAT mass after 10 days of treatment. However, the appearance of this tissue more closely resembled that of the thermogenically active IBAT from lean animals, having a deeper red-brown color and increased firmness. When both agents were adminis-

Table 1. Fasting Plasma Metabolites, Glucose Tolerance, Body Weight, and Food Consumption

Variable	Treatment				
	Lean (n = 7)	Control (n = 7)	PIO (n = 7)	CL (n = 7)	PIO + CL (n = 7)
Glucose (mg/dL)	104 ± 5*	117 ± 4	95 ± 2*	114 ± 4†	98 ± 3*
Insulin (μU/mL)	14 ± 3*	149 ± 18	65 ± 13*	57 ± 13*	55 ± 7*
FFA (mEq/L)	0.72 ± 0.04*	2.17 ± 0.25	0.90 ± 0.04*	1.37 ± 0.18*†	0.59 ± 0.04*
Glucose AUC‡	3620 ± 1270*	12440 ± 1600	3380 ± 230*	4200 ± 810*	7040 ± 2030*
Body weight final (g)	190 ± 4*	422 ± 16	444 ± 10†	380 ± 7*	392 ± 14
Δ Body weight (g)	15 ± 2*	31 ± 2	71 ± 3*†	14 ± 5*†	45 ± 5*
Food consumed§ (g/d)	14.3 ± 0.24*	23.3 ± 0.42	31.6 ± 1.3*†	19.2 ± 2.9	20.6 ± 2.6
Index of feeding efficiency‖	10.5 ± 1.3	13.2 ± 0.4	22.7 ± 1.0*	7.2 ± 2.6*†	21.9 ± 1.6*

NOTE. Data are the mean ± SE with the number of animals indicated in parentheses. Body weight and food consumption were monitored daily over the 10-day treatment period. Initial body weights of the obese groups were not statistically different from one another.

*Indicates significant differences from control, in which $P < .05$ using a 1-way ANOVA with Student Newman Kuel's post-ANOVA test.

†Indicates significant differences from PIO + CL, in which $P < .05$ using a 1-way ANOVA with Student Newman Kuel's post-ANOVA test.

‡Area under the glucose curve (AUC) from time 0 to 120 minutes (mg/min/dL) after an oral glucose challenge (1.35 g/kg).

§Daily food consumption per animal averaged over the 10-day period.

‖Feeding efficiency was determined for each animal and is expressed as the change in body weight over the 10-day period divided by the total food consumed.

Table 2. IBAT Composition

Treatment	Treatment Group				
	Lean (n = 7)	Control (n = 7)	PIO (n = 7)	CL (n = 7)	PIO + CL (n = 8)
IBAT mass (g)	0.24 ± 0.02*	1.70 ± 0.11	4.63 ± 0.55*†	1.78 ± 0.17†	3.03 ± 0.18*
Per mg wet tissue weight					
DNA (ng)	220 ± 20*	61 ± 5	70 ± 7†	127 ± 4*	135 ± 6*
Protein (μg)	77 ± 4*	25 ± 2	27 ± 3†	46 ± 2*	48 ± 3*
Citrate synthase (mU)	18.8 ± 0.7*	4.0 ± 0.9	4.4 ± 0.7†	8.1 ± 0.3*†	10.2 ± 0.8*
FAS Activity (pmol/min)	33.9 ± 5.5*	11.5 ± 0.7	15.7 ± 1.3‡	13.2 ± 0.9†	19.0 ± 1.5*
Per depot					
DNA (μg)	52 ± 2	103 ± 11	308 ± 17*†	228 ± 26*†	402 ± 15*
Protein (mg)	18 ± 0*	41 ± 4	117 ± 6*†	82 ± 7*†	143 ± 5*
Citrate synthase (U)	4.5 ± 0.3	6.5 ± 1.4	19.2 ± 2.3*†	14.7 ± 1.8*†	30.0 ± 1.6*
FAS activity (nmol/min)	8 ± 1	19 ± 2	71 ± 6*	24 ± 4†	58 ± 6*
Citrate synthase:FAS ratio	0.62 ± 0.08*	0.34 ± 0.06	0.28 ± 0.03†	0.65 ± 0.06*	0.57 ± 0.07*

NOTE. Data are the mean ± SE with the number of animals indicated in parentheses.
*Indicates significant differences from control in which P is $<.05$ using a 1-way ANOVA with Student Newman Kuel's post-ANOVA test.
†Indicates significant differences from PIO + CL, in which $P < .05$ using a 1-way ANOVA with Student Newman Kuel's post-ANOVA test.
‡Significantly different from control, Student's t test, $P < .02$.

tered in combination, IBAT mass and appearance were intermediate, relative to either treatment alone.

Composition of IBAT was assessed using biochemical markers (Table 2). When expressed per mg tissue wet weight, 10 days of PIO treatment did not alter IBAT DNA or protein concentrations, or citrate synthase activity (which is an indicator of carbon entry into the Kreb's cycle). Only FAS activity (a measure of fatty acid biosynthesis) was modestly elevated (37%) after PIO treatment. In contrast, 10 days of CL treatment doubled IBAT DNA, protein, and citrate synthase activity per mg tissue wet weight, without effecting FAS activity. IBAT taken from the combination treatment group had DNA and protein concentrations, and citrate synthase activity, similar to the CL treated group, and FAS activity similar to the PIO group, with no apparent drug-drug interactions (2-way ANOVA, not significant) on any of the measured parameters. When the size of the IBAT depot is taken into account, PIO treatment resulted in an increase in the total protein, DNA, citrate synthase, and FAS content, an effect due almost solely to an increase in depot mass, not a change in tissue composition. The effect of PIO and CL given in combination appeared to be additive on the total DNA, protein and citrate synthase content per IBAT depot, however, two-way ANOVA analysis showed no significant drug-drug interactions.

Electron micrographs (Fig 1) of IBAT from lean rats show characteristic brown adipocytes that contain multilocular lipid droplets surrounded by densely packed mitochondria. In contrast, adipocytes from control IBAT contained large unilocular

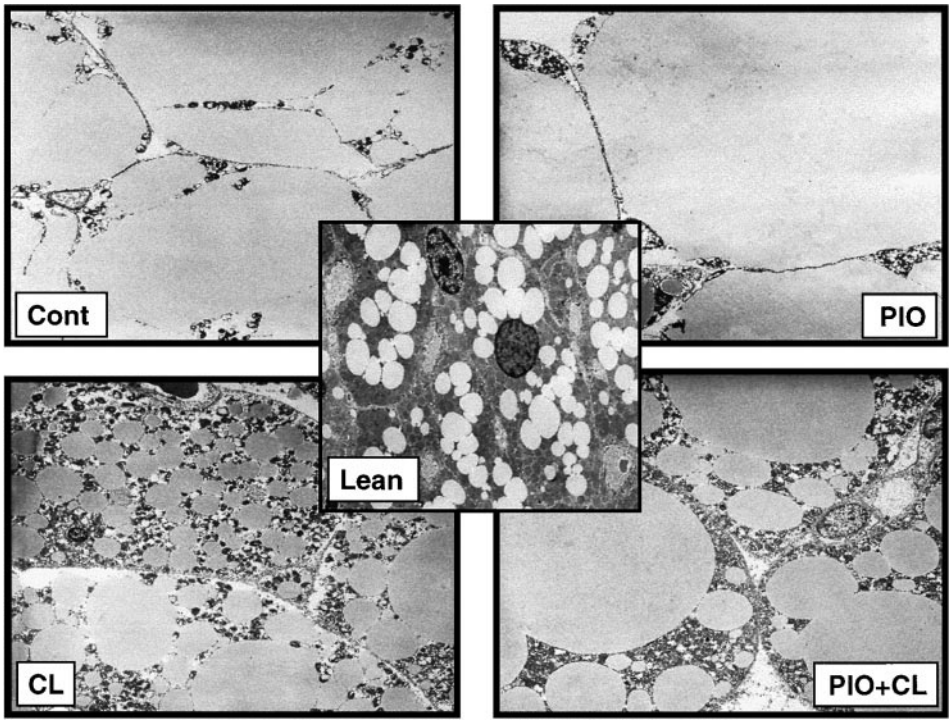

Fig 1. Effects of compound on IBAT morphology. After 10 days of treatment, IBAT tissues were fixed in osmium tetroxide, sectioned and electron micrographs taken. All tissues were taken from the center of the IBAT organ, and all images are the same magnification (1,100±). For comparison, lean IBAT is shown in the center.

lipid droplets with a thin layer of cytoplasm pushed against the plasma membrane, appearing much like adipocytes from WAT. PIO treatment did not alter the overall appearance of IBAT adipocytes, where the lipid deposition was still unilocular with no visible change in cytoplasmic deposition or mitochondrial content. The only PIO effect noted was a trend toward an increase in the size of these adipocytes. However, no size quantitation from the electron micrographs was performed. In contrast, IBAT from CL-treated rats was dramatically altered. These adipocytes contained multilocular lipid droplets surrounded by cytoplasm containing numerous mitochondria and had an overall appearance of IBAT similar to that of lean animals. The brown adipocytes from the combination-treated group were multilocular, but contained many larger lipid droplets surrounded by smaller droplets, that in some cases were fused, suggesting a dynamic state of lipid droplet conversion. These cells also had an increased number of visible mitochondria.

Further analysis of BAT adipocytes showed changes in cell size after treatment with both of these compounds (Fig 2). Ten days of PIO treatment modestly increased the number of small adipocytes (<30 μm in diameter) and also significantly right-shifted the entire midsized adipocyte population by 10 to 20 μm (peak range of control, 34 to 65 μm *v* PIO at 48 to 85 μm in diameter). No change in the distribution of large adipocytes (>100 μm diameter) was evident. These data suggest that PIO promotes IBAT adipocyte hypertrophy and adipogenesis. In contrast, 10 days of CL treatment resulted in a marked loss of the midsized adipocyte population (30 to 60 μm diameter), shifting the size distribution toward cells with a diameter of less than 30 μm, consistent with the generation of smaller fat cells through an increase in lipolysis and thermogenesis. Interestingly, CL had no effect on the large IBAT fat cell size (>100 μm) distribution. The profile for the combination-treated group (PIO + CL) was similar to the CL group, with the exception of a minor peak at 50 μm, consistent with the PIO-mediated appearance of larger fat cells.

While PIO increases IBAT mass, the above morphologic and biochemical data do not suggest a role for PIO in increasing IBAT thermogenic activity. When whole-body metabolic rates were assessed by indirect calorimetry after both 4 and 10 days of compound treatment (Table 3), PIO had no effect on whole body metabolic rates. In contrast, CL increased metabolic rates by 50% and 30% on days 4 and 10, respectively. Furthermore, PIO did not further enhance the actions of CL on whole body metabolism when the 2 compounds were administered together for 10 days. Consistent with these in vivo findings is the lack of an effect of PIO treatment on UCP1 mRNA levels in IBAT after 10 days of treatment (Fig 3). In comparison, 10 days of CL treatment doubled IBAT UCP1 mRNA levels. Similar results were seen after only 4 days of compound treatment, where PIO had no effect on UCP-1 mRNA (90 ± 14%, n = 4, not significant [NS] *v* control) and CL increased UCP-1 mRNA (187 ± 24%, n = 4, $P < .05$ *v* control). Leptin mRNA levels were unchanged with PIO treatment and were greatly diminished after CL treatment (Fig 3). The effect of CL to increase UCP-1 mRNA levels was blunted when administered in combination with PIO. In contrast, the CL-mediated decrease in leptin mRNA was unaffected with combined PIO + CL treatment. The

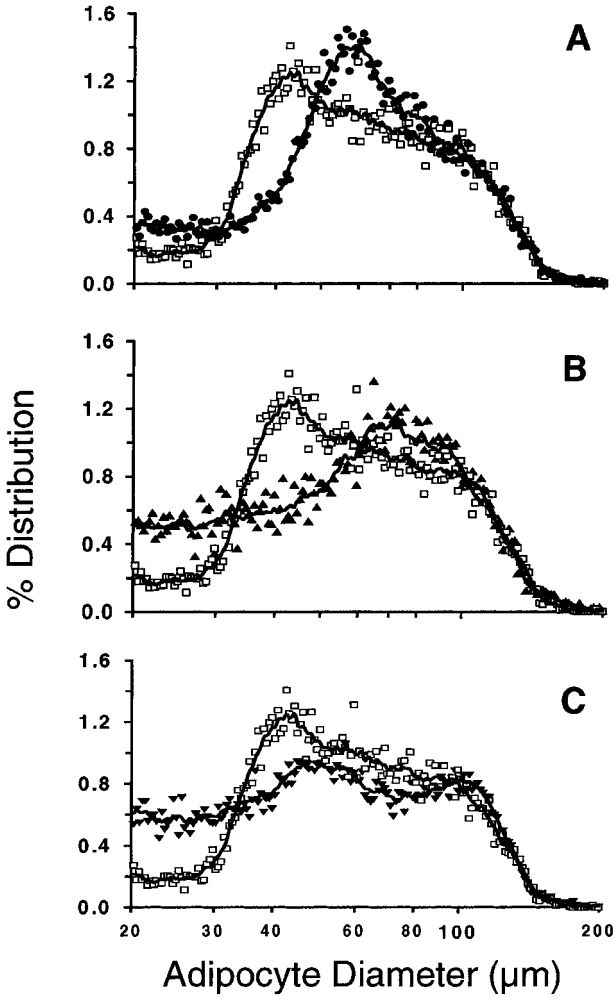

Fig 2. Brown adipocyte cell size profiles after 10 days of compound treatment. Obese fa/fa rats were treated with either vehicle (□, n = 4), PIO (●, n = 5), CL (▲, n = 5), or PIO + CL (▼, n = 6). Freshly isolated IBAT adipocytes were sized using a Coulter Multisizer II particle analyzer, and the size distribution of cells between 20 and 200 μm were expressed as a percent of total. Data are expressed as an averaged combined profile, fit with an adjacent-averaged curve.

levels of UCP1 were also assessed in both visceral and subcutaneous WAT depots, where UCP-1 signal was detectable only in visceral adipose tissue of CL-treated rats at levels 5% to 10% of control IBAT (data not shown). This is consistent with the appearance of brown adipocytes in WAT after β_3-adrenoceptor agonist treatment.[28,29]

DISCUSSION

While recent in vitro evidence[17-21] suggests that TZDs may mediate some of their antidiabetic effects by increasing energy expenditure, the studies herein clearly show that one respresentative TZD, PIO, does not increase metabolic rates and energy expenditure in an in vivo rodent model of obesity. When administered to obese *fa/fa* Zucker rats, PIO did not increase metabolic rates, even though IBAT mass was doubled. The increase in tissue mass was due predominantly to an increase in the size and number of lipid-laden adipocytes, resulting in a

Table 3. Whole Body Metabolic Rates (kcal/h)

	Treatment Group				
	Lean (n = 7)	Control (n = 7)	PIO (n = 7)	CL (n = 7)	PIO + CL (n = 8)
Day 4	0.67 ± 0.05*	1.50 ± 0.14	1.32 ± 0.05	2.28 ± 0.16*	ND
Day 10	1.73 ± 0.09*	2.05 ± 0.11	2.03 ± 0.13†	2.63 ± 0.14*	2.63 ± 0.09*

NOTE. Data represent the average of 5 readings and are the mean ± SEM with the number of animals indicated in parentheses. Energy expenditure measurements were performed during the light phase on day 4 and during the dark phase (scotophase) on day 10.

Abbreviation: ND, no data.

*Indicates significant differences from control in which $P < .05$ using a 1-way ANOVA with Student Newman Kuel's post-ANOVA test.

†Indicates significant differences from PIO + CL, in which $P < .05$ using 1-way ANOVA with Student Newman Kuel's post-ANOVA test.

tissue that is even whiter in appearance than that of IBAT taken from control animals. In contrast, CL increased thermogenesis and the effects on IBAT morphology were opposite, resulting in firmer, darker tissue containing smaller adipocytes with greater mitochondrial density, similar to IBAT from lean animals. These changes occurred without affecting IBAT mass and are consistent with the known ability of CL to increase the thermogenic capacity of IBAT.[11,12,16] Further evaluation showed that PIO, unlike CL, had no effect on IBAT UCP1 mRNA levels, consistent with the absence of an effect on metabolic rates. Treatment with CL resulted in a slower growth rate, which in the absence of a change in food consumption, is indicative of a decrease in feeding efficiency and is in keeping with its mechanism of action. Contrariwise, PIO-treated rats had a higher feeding efficiency, which in the face of unchanged whole-body metabolic rates, indicates an increase in energy storage and supports the observed increase in body weight gain.

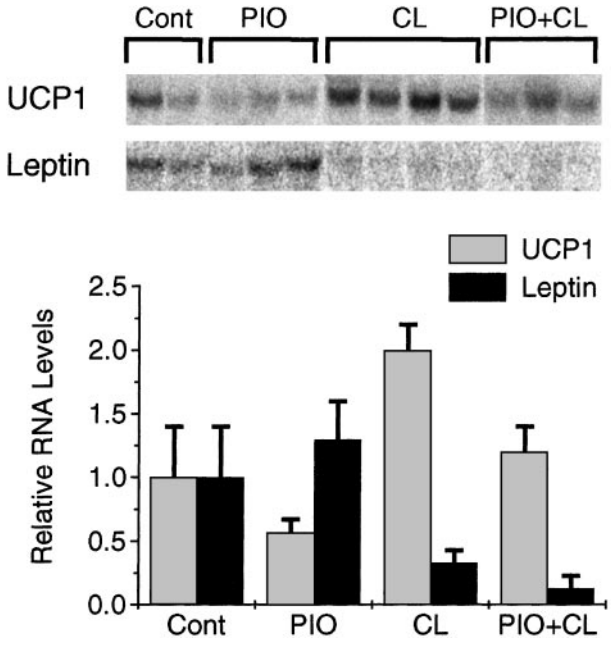

Fig 3. IBAT UCP1 and leptin steady-state mRNA levels. Total IBAT RNA was taken from obese *fa/fa* Zucker rats treated 10 days with either vehicle (Cont), pioglitazone (PIO), CL 316,243 (CL), or PIO + CL. (Top) Fractionated RNA (20 μg) was assessed for UCP1 and leptin mRNA levels by Northern blot analysis. (Bottom) The bands for UCP1 and leptin were quantitated and normalized relative to control levels (set equal to 1). The data are the mean ± SE of between 2 to 4 rats per group.

Overall, the effects of PIO in *fa/fa* Zucker rats are anabolic, consistent with the known adipogenic and lipogenic actions of TZDs, and do not support a role for promoting energy expenditure.

Several in vitro studies have shown that PPAR-γ agonists stimulate the differentiation of preadipocytes into mature UCP-1-containing brown adipocyte,[18-21] while in vivo, they result in an increase in IBAT mass.[17,18] Based on these observations, the assumption has been made that PPAR-γ agonists mediate their antidiabetic effects, at least in part, through an increase in BAT/UCP1-mediated thermogenesis. While the data from these studies support the findings of an increase in IBAT mass, they clearly show the lack of an effect on whole-body metabolic rates or IBAT morphology that would be suggestive of increased thermogenesis. The PIO-induced increase in IBAT mass appears to be due to both a hypertrophic and hyperplasic effect, because the total DNA content per IBAT depot is 3 times that of controls (308 *v* 103 μg DNA/depot), while still maintaining large unilocular adipocytes. This effect is most likely due to DNA replication and clonal expansion of preadipocytes in IBAT, consistent with the known early events of adipogenesis,[30] and increased lipid biosynthesis. Based on the absence of any elevation in UCP1 mRNA levels, it can be inferred that these new adipocytes are more like those found in WAT, a premise that is consistent with the functional atrophy of IBAT in *fa/fa* Zucker rats. The increase in tissue DNA content could also be due to a disproportional increase in the number of stromal-vascular cells. However, because the DNA content per milligram tissue wet weight did not change, this is an unlikely possibility.

Another indication of the atrophied state of *fa/fa* IBAT is the relatively high levels of leptin expression, considered a white adipose-specific marker. The leptin expression in this obese animal model may come from brown adipocytes that are lipid-laden, expressing ''white adipocyte-like'' genes. Alternatively, it may come from white adipocytes located within the brown adipose depot, contributing to the increased IBAT mass. After CL treatment, IBAT leptin expression is dramatically reduced, consistent with this tissue becoming more ''brown'' and thermogenically active. However, after PIO treatment, leptin mRNA levels remain unchanged. Interestingly, it has recently been shown that cultured brown preadipocytes can be terminally differentiated with insulin and dexamethasone into lipid containing adipocytes that lack thermogenic capacity.[31] These cells have significant lipid deposition and lipolytic capacity, but lack detectable UCP1 protein. Thus, it is likely that PIO promotes both the hypertrophy of existing brown adipo-

cytes and stimulates the proliferation and differentiation of preadipocytes, giving rise to new adipocytes within the IBAT that are more white than brown in phenotype and function. Taken together, these results suggest that terminal differentiation of brown adipocytes can be dissociated from thermogenic activity, and that PIO promotes IBAT adipogenesis and lipogenesis, contributing to the overall increase in the mass of this tissue without affecting energy expenditure.

Further biochemical evidence that PIO promotes lipid storage, while CL promotes its utilization, comes from the observed effects of these treatments on citrate synthase and FAS activity (Table 2). In BAT, the activity of citrate synthase indicates the flux of 2 carbon intermediates into the TCA cycle, resulting in the production of citrate. Citrate either continues through the TCA cycle for further oxidation or is exported to the cytoplasm where it is converted to acetyl CoA and used for fatty acid biosynthesis. Thus, a high citrate synthase to FAS ratio favors oxidation, and a low ratio favors lipid biosynthesis. After PIO treatment, the levels of FAS activity per milligram wet tissue weight in IBAT were increased without altering citrate synthase activity or markers of overall cellularity (DNA and protein content). As well, the citrate synthase to FAS ratio was no different than controls. This indicates that PIO increased fatty acid biosynthesis without increasing the flux of 2 carbon intermediates into the TCA cycle or dramatically altering the tissue cellularity. Such a profile is consistent with thermogenically inactive brown adipose tissue storing more triglyceride. In contrast, CL had the opposite effect, doubling BAT DNA and protein content and citrate synthase activity, and increasing the citrate synthase to FAS ratio to those of lean animals. This is consistent with the known effects of this agent to increase thermogenic activity in brown adipose tissue. When PIO and CL were administered together, the PIO effects on FAS activity dominated, whereas the effects on citrate synthase activity were synergistic, suggesting a modest increase in the overall utilization of 2 carbon intermediates, that may, in part, be directed toward fatty acid biosynthesis.

While the data from these studies do not support a role for TZDs in stimulating thermogenesis, it is possible that the genotype of obese *fa/fa* Zucker rat may mask the potential thermogenic effects of the thiazolidinediones, effects that would otherwise occur in normal rodents. The *fa/fa* mutation is associated with a myriad of physiologic abnormalities that contribute to the obese phenotype of these animals. For example, the inability of PIO to activate the IBAT and enhance thermogenesis might be a consequence of the lower sympathetic tone[32] in these obese animals. However, this is unlikely because CL effectively activates IBAT, and when given in combination with CL, PIO does not promote any further increase in energy expenditure from the CL-activated IBAT, although it is as efficacious as CL in promoting antidiabetic effects. Similarly, the lack of a thermogenic effect of PIO cannot be attributed to the lack of an intact leptin pathway because TZDs have been documented to increase IBAT mass even in animals with an intact leptin signaling loop.[20] Thus, the ability of PIO to promote antidiabetic effects in the absence of any increase in metabolic rate suggests that the mechanism(s) through which it mediates its therapeutic benefit do not include IBAT thermogenesis and increased whole body energy expenditure. It is also unlikely a function of the animal model used in these studies. Hyperphagia and lower metabolic rates are phenotypic characteristic of *fa/fa* Zucker animals, resulting in higher metabolic efficiencies and obesity.[33,34] Treatment of these animals with PIO further enhances their metabolic efficiency resulting in the storage of an even greater proportion of the food they consume. The increased IBAT mass (Fig 1), approximately 3 g, accounts for less than 10% of the increase in total body weight ($\simeq$40 g). Body composition studies indicate that the PIO-induced increase in body weight in obese *fa/fa* rats is due primarily to lipid accretion.[35] Further studies aimed at providing a more detailed analysis of the effects of PIO on WAT morphology and physiology and the role of this tissue in mediating the antidiabetic effects of PIO are ongoing.

Both PIO and CL are very effective at lowering plasma FFA levels in this hyperlipidemic rodent model, albeit via different mechanistic pathways. Similar lipid lowering effects have been observed in several other diabetic models after treatment with these agents.[10,16,36] Considering the evidence that implicates disturbed FFA metabolism in the development of insulin resistance,[37-40] pharmacologic agents that decrease excessive FFA exposure on peripheral tissues are expected to provide therapeutic benefit by improving insulin sensitivity and augmenting glucose disposal.[5] Hence, the antidiabetic effects of these 2 agents, with very different mechanisms of action, are probably a function of their common ability to dramatically redirect FFA metabolism. Overall, these studies show that PIO and CL are very effective antidiabetic agents, but unlike CL, the antidiabetic effects of PIO are not mediated via an activation of IBAT thermogenesis and enhanced whole body metabolism. Instead, and contrary to the known relationship between obesity and insulin resistance, the antidiabetic effects of PIO occur in the presence of an increase in metabolic efficiency and whole body adiposity. This suggests that the antidiabetic effects of TZDs might be a function of their ability to lower plasma FFA levels through increased energy storage.

ACKNOWLEDGMENT

The authors would like to thank Xilin Liu for technical assistance in IBAT tissue collection, Catherine Crisafi for the insulin radioimmunoassays, and Craig Isaacson for providing the mouse leptin cDNA. CL 316,243 was a gift from Dr Kurt Steiner, Wyeth Ayerst, Princeton, NJ.

REFERENCES

1. Saltiel AR, Olefsky JM: Thiazolidinediones in the treatment of insulin resistance and type II diabetes. Diabetes 45:1661-1669, 1996

2. Willson TM, Cobb JE, Cowan DJ, et al: The structure-activity relationship between peroxisome proliferator-activated receptor-γ agonism and the antihyperglycemic activity of thiazolidinediones. J Med Chem 39:665-668, 1996

3. Schoonjansm K, Staels B, Auwerx J: The peroxisome proliferator activated receptors (PPARs) and their effects on lipid metabolism and adipocyte differentiation. Biochem Biophys Acta 1302:93-109, 1996

4. Spiegelman BM: PPAR-γ: Adipogenic regulator and thiazolidinedione receptor. Diabetes 47:507-514, 1998

5. Foley JE, Anderson RC, Bell PA, et al: Pharmacologic strategies for reduction of lipid availability. NY Acad Sci 827:231-245, 1997

6. Yoshioka S, Nishino H, Shiraki T, et al: Antihypertensive effects of CS-045 treatment in obese Zucker rats. Metabolism 42:75-80, 1993

7. Fujiwara T, Wada M, Fukuda K, et al: Characterization of CS-045, a new oral antidiabetic agent, II. Effects on glycemic control and pancreatic islet structure at a late stage of the diabetic syndrome in C57BL/KsJ-db/db mice. Metabolism 40:1213-1218, 1991

8. de Souza CJ, Yu JH, Robinson DD, et al: Insulin secretory defect in Zucker *fa/fa* rats is improved by ameliorating insulin resistance. Diabetes 44:984-991, 1995

9. Hallakou S, Doaré L, Foufelle F, et al: Pioglitazone induces *in vivo* adipocyte differentiation in the obese Zucker *fa/fa* rat. Diabetes 46:1393-1399, 1997

10. Ikeda H, Taketomi S, Sugiyama Y, et al: Effects of pioglitzone on glucose and lipid metabolism in normal and insulin resistant animals. Arzneim-Forsch Drug Res 40:156-162, 1990

11. Danforth E Jr, Himms-Hagen J: Obesity and diabetes and the beta-3 adrenergic receptor. Eur J Endocrinol 136:362-365, 1997

12. Himms-Hagen J, Cui J, Danforth E Jr, et al: Effects of CL-316,243, a thermogenic β_3-agonist, on energy balance and brown and white adipose tissue in rats. Am J Physiol 266:R1371-R1382, 1994

13. Yoshida T, Sakane N, Wakabayshi Y, et al: Anti-obesity and anti-diabetic effects of CL 316,243, a highly specific β_3-adrenoceptor agonist, in yellow KK mice. Life Sci 54:491-498, 1994

14. Umekawa T, Yoshida T, Sakane N, et al: Anti-obesity and anti-diabetic effects of CL 316,243, a highly specific β_3-adrenoceptor agonist, in Otsuka Long-Evans Tokushima Fatty rats: Induction of uncoupling protein and activation of glucose transporter 4 in white fat. Eur J Endocrinol 136:429-437, 1997

15. de Souza CJ, Hirshman MF, Horton ES: CL-316,243, a β_3-specific adrenoceptor agonist, enhances insulin-stimulated glucose disposal in nonobese rats. Diabetes 46:1257-1263, 1997

16. Liu X, Perusse F, Bukowiecki LJ. Mechanisms of the antidiabetic effects of the beta 3-adrenergic agonist CL-316243 in obese Zucker-ZDF rats. Am J Physiol 274:R1212-R1219, 1998

17. Foellmi-Adams LA, Wyse BM, Herron D, et al: Induction of uncoupling protein in brown adipose tissue. Biochem Pharmacol 52:693-701, 1996

18. Paulik MA, Lenhard JM. Thiazolidinediones inhibit alkaline phosphate activity while increasing expression of uncoupling protein, deiodinase, and increasing mitochondrial mass in C3H10T1/2 cells. Cell Tissue Res 290:79-87, 1997

19. Digby JE, Montague CT, Sewter CP, et al: Thiazolidinedione exposure increases the expression of uncoupling protein 1 in cultured human preadipocytes. Diabetes 47:138-141, 1998

20. Tai TAC, Jennermann C, Brown KK, et al: Activation of the nuclear receptor peroxisome proliferator-activated receptor γ promotes brown adipocyte differentiation. J Biol Chem 271:29909-29914, 1996

21. Aubert J, Champigny O, Saint-Marc P, et al: Up-regulation of UCP-2 gene expression by PPAR agonists in preadipose and adipose cells. Biochem Biophys Res Commun 238:606-611, 1997

22. Weir BJ: New methods for calculating metabolic rate with special reference to protein metabolism. J Physiol 109:1-9, 1949

23. Rodbell M: Metabolism of isolated fat cells. J Biol Chem 239:375-380, 1964

24. Kashiwagi A, Verso MA, Andrews J, et al: *In vitro* insulin resistance of human adipocytes isolated from subjects with noninsulin-dependent diabetes mellitus. J Clin Invest 72:1246-1254, 1983

25. Srere PA, Brazil H, Gonen L: The citrate condensing enzyme of pigeon breast muscle and moth flight muscle. Acta Chem Scand 17:S129-S134, 1963 (suppl 1)

26. Lynen F: Yeast fatty acid synthase. Methods Enzymol 14:17-33, 1969

27. Claycombe KJ, Jones BH, Standridge MK, et al: Insulin increases fatty acid synthase gene transcription in human adipocytes. Am J Physiol 274:R1253-R1259, 1998

28. Ghorbani M, Himms-Hagen J: Appearance of brown adipocytes in white adipose tissue during CL 316,243-induced reversal of obesity and diabetes in Zucker *fa/fa* rats. Int J Obes Relat Metab Disord 21:465-475, 1997

29. Guerra C, Koza RA, Yamashita H, et al: Emergence of brown adipocytes in white fat in mice is under genetic control: Effects on body weight and adiposity. J Clin Invest 102:412-420, 1998

30. MacDougald OA, Lane MD: Transcriptional regulation of gene expression during adipocyte differentiation. Ann Rev Biochem 64:345-373, 1995

31. Klaus S, Ely M, Encke D, et al: Functional assessment of white and brown adipocyte development and energy metabolism in cell culture. J Cell Sci 108:3171-3180, 1995

32. Jeanreneaud B: Neuroendocrinology and evolutionary aspects of experimental obesity, in Oomura Y, Tarui S, Inoue S, et al (eds): Progress in Obesity Research. Montrouge, France, Libbey, 1990, pp 409-421

33. Argiles JM: The obese Zucker rat: A choice for fat metabolism 1968-1988: Twenty years of research on the insights of the Zucker mutation. Prog Lipid Res 28:53-66, 1989

34. Pullar JD, Webster AJ: The cost of fat and protein deposition in the rat. Br J Nutr 37:355-363, 1977

35. Meglasson M, de Souza C, Yu J, et al: Effects of thiazolidinedione insulin sensitizer on growth and body composition of Zucker rats. Diabetes 42:240A, 1995 (abstr, suppl 1)

36. Sugiyama Y, Taketomi S, Shimura Y, et al: Effects of pioglitazone on glucose and lipid metabolism in Wistar fatty rats. Arzneimittelforschung 40:263-267, 1990

37. Roden M, Price TB, Perseghin G, et al: Mechanism of free fatty acid-induced insulin resistance in humans. J Clin Invest 97:2859-2865, 1996

38. Kruszynska YT: The role of fatty acid metabolism in the hypertriglyceridemia and insulin resistance of type 2 (non-insulin dependent) diabetes, in Marshall SM, Home PD, Rizza RA (eds): The Diabetes Annual. New York, NY, Elsevier, 1995, pp 107-139

39. Bergman RN: New concepts in extracellular signaling for insulin action: The single gateway hypothesis. Recent Prog Horm Res 52:357-387, 1997

40. Boden G: Role of fatty acids in the pathogenesis of insulin resistance and NIDDM. Diabetes 45:3-10, 1997